Molecular Therapy
Nucleic Acids
Original Article

# Single-stranded HDR templates with truncated Cas12a-binding sequences improve knock-in efficiencies in primary human T cells

Ana-Maria Nitulescu,[1,2] Weijie Du,[1,2] Viktor Glaser,[1,2] Jonas Kath,[1,2,7] Eric J. Aird,[3] Grégoire Cullot,[3] Robert Greensmith,[4,5] Nanna Steengaard Mikkelsen,[6] Maik Stein,[1,2] Rasmus O. Bak,[6] Michael Kaminski,[4,5] Jacob E. Corn,[3] and Dimitrios L. Wagner[1,2,7,8,9]

[1]Berlin Center for Advanced Therapies, Charité – Universitätsmedizin Berlin, Corporate Member of Freie Universität Berlin, Humboldt-Universität zu Berlin, and Berlin Institute of Health, 13353 Berlin, Germany; [2]Berlin Institute of Health Center for Regenerative Therapies, Berlin Institute of Health at Charité–Universitätsmedizin Berlin, 13353 Berlin, Germany; [3]Department of Biology, Institute of Molecular Health Sciences, ETH Zurich, Zurich, Switzerland; [4]Berlin Institute for Medical Systems Biology (BIMSB), Max Delbrück Center for Molecular Medicine in the Helmholtz-Association, 10115 Berlin, Germany; [5]Department of Nephrology and Medical Intensive Care, Charité - Universitätsmedizin Berlin, Medizinische Klinik m.S. Nephrologie und Intensivmedizin, 10117 Berlin, Germany; [6]Department of Biomedicine, Aarhus University, 8000 Aarhus, Denmark; [7]Center for Cell and Gene Therapy, Baylor College of Medicine, Houston, TX 77030, USA; [8]Department of Molecular and Cellular Biology, Baylor College of Medicine, Houston, TX 77030, USA; [9]Dan L. Duncan Comprehensive Cancer Center, Baylor College of Medicine, Houston, TX 77030, USA

**CRISPR-Cas12a gene editing offers an alternative to Cas9-based methods, providing better targeting of AT-rich regions, simplified guide RNA manufacturing, and high specificity. However, the efficacy of donor-based editing is subject to various factors, with template format playing a crucial role. Currently, the predominant non-viral template format for homology-directed repair (HDR) after nuclease-induced DNA breaks is double-stranded DNA, which is toxic when transfected at high doses. Others have demonstrated that using single-stranded DNA (ssDNA) with flanking double-stranded Cas-target-sequences (CTS) as a template for Cas9-mediated gene editing can mitigate this toxicity and increase knock-in efficiency. Here, we investigate CTS design for AsCas12a Ultra by exploring PAM orientation and binding requirements. Additionally, we rule out ssDNase activity of AsCas12a under cell-physiological $Mg^{2+}$ conditions. Finally, we showcase the advantage of ssDNA donors with CTS (ssCTS) at high doses for delivering clinically relevant transgenes of varying sizes into three TCR-CD3 complex genes (*TRAC*, *CD3ζ*, *CD3ε*), achieving up to 90% knock-in rates for a 0.8kb-insert at the *CD3ε* locus. Long-read sequencing confirmed higher HDR rates and revealed that CTS reduced partial integration events compared to unmodified ssDNA. Overall, AsCas12a and ssCTS represent a platform for highly efficient knock-in in primary human T cells with minimal toxicity.**

## INTRODUCTION

Adoptive transfer of engineered T cells expressing synthetic antigen receptors, such as chimeric-antigen receptors (CARs), is an effective approach for second- or third-line treatment for B cell malignancies.[1,2] Currently, all approved CAR-T cell products are manufactured in an autologous (personalized) fashion and employ nontargeted gene transfer of transgenes using retro- or lentiviral vectors. However, this process is associated with significant expenses. Production and testing of clinical grade viral vectors contributes to high material costs, especially at early clinical phases.[3] To reduce these costs, clinical trials have commenced using CAR-T cells produced with non-viral transposase systems. Like retroviruses, transposases integrate their cargo semi-randomly into the chromosomes, and in the case of a hyperactive version of the transposase piggyBac, this has contributed to the development of CAR-positive T cell malignancies.[4] Therefore, there is a need to develop and optimize non-viral gene transfer, which avoids risks associated with random integration.

Precise genomic integration of CAR transgenes can enhance the quality of cell products to predictable transgene expression levels,[5] and it may further improve the safety of the cellular product by reducing the risk of insertional mutagenesis.[4,6] Furthermore, while randomly integrating vectors depend on exogenous promoter-driven transgene expression, gene editing can harness endogenous gene regulation to enhance product potency. For instance, knock-in into the *T cell receptor (TCR) Alpha Constant* (*TRAC*) locus has been shown to improve CAR-T cell potency and persistence in preclinical mouse models of B cell acute lymphoblastic leukemia

Received 3 October 2024; accepted 14 May 2025;
https://doi.org/10.1016/j.omtn.2025.102568.

**Correspondence:** Dimitrios L. Wagner, M.D., Ph.D., Berlin Center for Advanced Therapies, Charité – Universitätsmedizin Berlin, Corporate Member of Freie Universität Berlin, Humboldt-Universität zu Berlin, and Berlin Institute of Health, 13353 Berlin, Germany.
**E-mail:** dimitrios-l.wagner@charite.de

(B-ALL).[7] Ongoing clinical studies are investigating the potency of *TRAC*-replaced CAR-T cells in treatment-refractory large B cell lymphoma.[8] Gene editing of other TCR/CD3 complex genes, such as *CD3ζ* and *CD3ε*, has also been proposed to create potent CAR-T cells[5,9] as well as TCR fusion constructs (TRuC).[10–12] We previously demonstrated that *CD3ε* gene editing with TRuC is a strategy uniquely suited for redirection of immunosuppressive immune cells, called regulatory T cells (Tregs).[13] Reprogramming Tregs to recognize alloantigens, such as HLA-A2, holds significant potential to suppress allo-mediated rejection in solid organ transplantation[14] and reduce or replace hazardous long-term immunosuppression in patients. Consequently, gene editing is a promising gene transfer modality to manufacture redirected T cell products with enhanced fitness for diverse medical applications.

The efficacy of site-specific gene transfer using CRISPR-Cas gene editing depends on various factors, such as the targeted locus, the specific programmable nuclease, guide RNA (gRNA) selection, and the homology-directed repair template (HDRT).[15,16] Adenovirus-associated virus (AAV) vectors represent the current gold-standard template for HDR in T cells as they can achieve high levels of integration. However, AAV vector production is complex and expensive for clinical use. The most commonly used non-viral template formats include plasmids,[17–22] linear double-stranded DNA (dsDNA),[5,23–29] and single-stranded DNA (ssDNA).[23,30,31] Previous studies have shown that electroporation of cells with ssDNA exhibits reduced cell toxicity compared to dsDNA templates.[23] However, aside from the use of small single-stranded oligonucleotides (ssODNs) for point mutation repair and smaller inserts,[32] knock-in rates using ssDNA for larger transgenes are generally low.[33] To boost CRISPR-Cas9 editing efficacy with ssDNA, Shy et al. proposed to integrate truncated Cas-target-sequences (tCTS) into the ends of ssDNA HDRTs.[34] These sequences are intended to enhance template delivery into the nucleus by serving as binding sites for the Cas9 protein, which contains nuclear localization signals (NLS).[24] The truncated format of the CTS is designed to prevent Cas-mediated cleavage of the template. To date, ssDNA with double-stranded tCTS (ssCTS) has not been adapted from the Cas9 system to other programmable nucleases.

In addition to considering the HDRT format, careful selection of the nuclease is warranted to ensure compatibility and efficient DNA double-stranded break (DSB) induction within the target region. Given that most mammalian genes are GC-rich, the presence of the requisite 5′-NGG-3′ protospacer adjacent motif (PAM) enables targeting *Streptococcus pyogenes* Cas9 (SpCas9) to specific locations. This, coupled with the high efficacy and extensive characterization of the enzyme,[35–37] has established SpCas9 as the preferred choice for genome editing. However, alternative nucleases like *Acidaminococcus species* Cas12a (AsCas12a) present advantageous properties over SpCas9 for specific applications.[38] Unlike SpCas9, AsCas12a creates staggered-end DSBs distal from a T-rich PAM, which helps guide the precise alignment of complementary DNA sequences during HDR.[38,39] Moreover, the nuclease operates effectively with only a short single crRNA of 42 nucleotides, combining the roles of both crRNA and tracrRNA, which is easier to manufacture via solid state synthesis than gRNAs of 100-nucleotide length required for SpCas9 gRNA.[40] Furthermore, studies have shown that AsCas12a is less tolerant for mismatches than SpCas9, thereby reducing unintended off-target effects.[40,41] Despite its advantages, the widespread adoption of Cas12a as a genome editing tool has been hindered by its comparatively lower editing efficiency in living cells.[42] To address this limitation, Zhang et al. developed an enhanced version of Cas12a, known as AsCas12a Ultra, by introducing two-point mutations, M537R and F870L, to boost its activity.[43] Their study demonstrated that these mutations significantly improved efficacy while maintaining the high intrinsic dsDNA-specificity of the nuclease. Previous studies demonstrated that both LbCas12a and AsCas12a enzymes can display indiscriminative ssDNase function *in vitro*—a function that is activated following successful cleavage of the dsDNA target.[44,45] This feature has sparked the development of *in vitro* diagnostic assays[46]; however, it could be detrimental for genome editing efficiency with ssDNA HDRTs due to donor degradation *in cellulo*. It is unclear whether AsCas12a Ultra shares this feature of other Cas12a enzymes. Consequently, AsCas12a Ultra offers a putative alternative to SpCas9 that has the potential to expand the therapeutic genome editing landscape, although the ssDNase activity could represent a caveat for its use with ssDNA HDRTs. In this study, we demonstrate highly efficient virus-free gene editing of T cells using modified ssDNA templates and AsCas12a Ultra.

First, we examined various AsCas12a-binding motifs as end modifications in dsDNA templates. After optimization of dsDNA templates, we incorporated different promising CTS-motifs into ssDNA HDRTs. We investigated whether a previously described $Mg^{2+}$-dependent ssDNase activity of the AsCas12a[44] could lead to undesired degradation of ssDNA HDRTs *in vitro*. Digestion assays demonstrated that neither intact nor truncated CTS-modified ssDNA templates were digested under physiological $Mg^{2+}$ concentrations. Finally, we assessed the HDR efficacy and toxicity of different non-viral DNA templates (dsDNA or ssDNA with or without CTS) encoding clinically relevant transgenes for cancer, autoimmune disorders, and transplantation medicine. Regardless of the transgene or the specific locus, using ssCTS and AsCas12a exhibited improved HDR efficiencies by 3- to –10-fold over unmodified ssDNA and sustained high cell viability even at the highest template concentration employed. Resulting T cells remained functional. Long-read sequencing of the on-target locus confirmed higher CAR integration and reduced undesired integration events of ssCTS over unmodified linear ssDNA HDRTs. We demonstrate that AsCas12a Ultra and ssDNA with appropriate CTS modifications may be used to optimize manufacturing of CAR/TCR-redirected T cell products.

## RESULTS

### Flanking truncated Cas9 target sequences enhance ssDNA-mediated CD19-CAR insertion at the *TRAC* locus

To validate reported effects of tCTS-modified ssDNA HDRTs in primary human T cells, we performed non-viral knock-in experiments

with a 2-kb-sized second-generation CD19-CAR (2.8 kb including homology arms [Has]) for targeted integration into the *TRAC* locus using the previously described SpCas9 CTS design.[34] For this, we generated ssDNA from the sense (+) and antisense (−) strand and incorporated tCTS on either the 5′ or 5′ and 3′ ends (Figure S1A). The CTS motifs included a 4-bp buffer sequence, a truncated sgRNA target sequence (with 6-bp mismatches [mm]) and a PAM "In" orientation (facing toward the insert). Prior to electroporation, corresponding oligodeoxynucleotides (ODNs) were hybridized to the CTS to create dsDNA ends. Using our CRISPR-Cas9 gene editing protocol without any HDR enhancers,[28] we examined the impact of various ssCTS designs on gene insertion rates and the number of transgene-expressing T cells 4 days post-electroporation with 0.5 μg of DNA using flow cytometry (Figure S1B). Consistent with prior findings,[34] ssCTS HDRTs performed better than non-modified ssDNA, likely attributed to enhanced CTS-facilitated DNA nuclear delivery (Figure S1C). In contrast to the previous report, we found that modifications both at the 5′ and 3′ end yielded higher HDR frequencies than ssDNA-HDRTs with just a single 5′-tCTS (Figure S1C). Furthermore, compared to conventional dsDNA templates, ssCTS HDRTs with flanking modifications demonstrated comparable HDR efficiencies and knock-in cell counts, with antisense ssCTS yielding higher HDR frequencies and knock-in cell numbers than sense ssCTS. Taken together, the generation of ssDNA from the antisense strand and the inclusion of CTS modifications on both DNA ends resulted in the highest knock-in rates (mean 23% ± SD 10.5) with the SpCas9-nuclease.

### Reduced crRNA mismatches and PAM "In" orientation of Cas12a target sequence motifs enhance dsCTS knock-in efficacy

We reasoned that the same strategy of using CTS to enhance SpCas9 editing[24] could be adapted to the AsCas12a nuclease. To this end, we first set out to test different CTS configurations using dsDNA HDRTs. We designed CTS motifs specific for Cas12a that included a 16-bp buffer sequence, a PAM, and either an intact or truncated crRNA target sequence (Figure 1A). Given the previously reported low intrinsic tolerance of AsCas12a for mismatches within regions proximal (1–18 bp) to the PAM,[40,43] we tested crRNA target sequences with 0, 2, 4, 6, 8, and 12-bp mismatches distal to the PAM. Moreover, we investigated the impact of the orientation of the gRNA-recognition sequence by placing the PAM either "In" (red) or "Out" (blue) of the templates (facing inward or outward in relation to the insert). The impact of the CTS motifs on knock-in efficiency was then compared in terms of the relative HDR frequency (measured by flow cytometry) and the number of transgene-expressing cells relative to unmodified dsDNA (Figure 1B). To exclude construct- or locus-specific bias, we conducted a screening of the different CTS motifs in HDRTs for three different knock-in strategies, designed to introduce CAR transgenes of different sizes at three distinct loci of the T cell receptor complex. These included a 0.8kb-sized HLA-A2-specific TRuC at the *CD3ε*-locus (smallest transgene), a 1kb-sized truncated CD19-CAR at the *CD3ζ*-locus, or a complete 2kb-sized CD19-CAR at the *TRAC*-locus (largest transgene) (Figure 1C).

With dsDNA HDRTs, CTS modifications with PAM "In" and lower number of mm increased the relative knock-in rates over unmodified dsDNA HDRTs. The relative increases in HDR frequencies were more evident for smaller than for the largest HDRT. For the *CD3ε*-directed HDRT containing the smallest insert (0.8kb-HLA-A2-TRuC), the inclusion of CTS with PAM "In" (and up to 6 mismatches) resulted in up to a 4.5-fold increase in HDR efficiency of dsCTS relative to dsDNA (Figure 1C, top panel). Similarly, for the *CD3ζ*-directed 1-kb-CD19-CAR HDRT (1.8 kb including HAs), the addition of CTS PAM "In" also enhanced HDR efficacy in some conditions, such as CTS PAM "In" 0-, 2-, and 4-bp mismatches (mm) (Figure 1C, middle panel). For instance, templates with a 4-bp-mm CTS PAM "In" demonstrated on average a 4-fold increase (± SD 1.48) in HDR frequencies compared to dsDNA. In the case of the *TRAC*-directed 1.8-kb-CD19-CAR (2.6 kb including HAs), increased knock-in rates were less pronounced and were only observed with CTS PAM "In" templates with the least number of mm (Figure 1C, bottom panel). For example, dsCTS with a 2-bp mm and a PAM "In" orientation showed on average an increase in HDR efficiency of 1.4-fold (± SD 0.2). The number of transgene-positive T cells was only increased in conditions with the *CD3ζ*-HDRT with CTS PAM "In" and few mismatches. In all other conditions and HDRTs, the relative increases in HDR frequencies did not result in higher edited T cell yields (Figure 1C). Overall, relative improvements of CRISPR-Cas12a-mediated knock-in rates were most pronounced when utilizing templates with fewer crRNA mm ranging from 0 to 4 and a PAM "In" orientation in the CTS region. These designs were further evaluated in the ssCTS format.

### Flanking double-stranded CTS improves HDR efficiency of ssDNA without inducing ssDNase activity of AsCas12a under physiological magnesium concentrations

Inclusion of dsDNA CTS end modification in ssDNA HDRTs could trigger unspecific DNase activity after binding of the AsCas12a-crRNA complex to its target (the CTS) *in vitro* (prior to electroporation into the T cells) or *in cellulo* (after electroporation). To evaluate the propensity of AsCas12a Ultra to degrade ssDNA HDRTs with CTS *in vitro*, we generated ssDNA from the antisense strand and incorporated CTS on both ends (Figure 2A). The CTS motifs included a 4-bp buffer sequence, a complete or 4-bp mm crRNA target sequence and a PAM "In" orientation. To assess whether AsCas12a indiscriminately degrades ssCTS templates, the HDRTs were co-incubated with the crRNA-nuclease complex employed in electroporation experiments. This was performed at 37°C for 30 min with or without the NEB2 buffer containing a high concentration of $Mg^{2+}$, which served as a positive control since it activates Cas12 to indiscriminately degrade ssDNA even without the presence of a crRNA[44] (Figure 2B, left side). Non-specific nuclease activity was detected solely in the presence of high $Mg^{2+}$, independent of the crRNA (Figure 2B, right side). Moreover, the inclusion of either complete or truncated CTS did not affect the nonspecific cleavage activity of

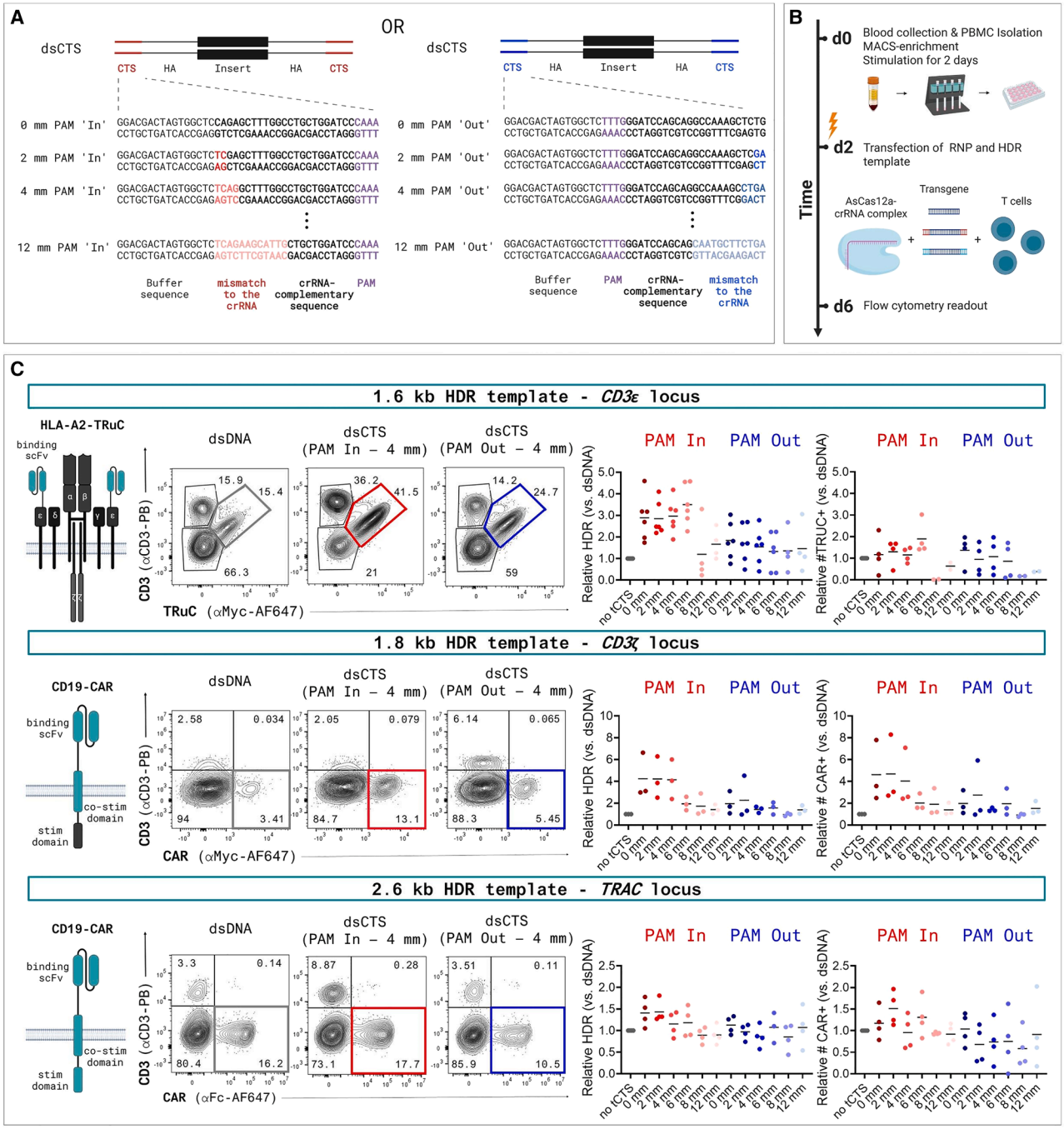


**Figure 1. Cas12a target sequence motifs with fewer crRNA mismatches (mm) and PAM "In" orientation increase knock-in efficiency of dsDNA CAR or TRuC constructs independent of the edited locus**

Virus-free insertion of an HLA-A2-TRuC and two CD19-CAR transgenes into the human *TRAC*, *CD3ζ*, or *CD3ε* loci. (A) Designs of dsCTS donor templates are shown. The inserts are flanked by HAs with additional AsCas12a CTS. These include a 16-bp buffer region, a PAM, and either an intact (CTS with 0-bp mm) or a truncated crRNA sequence (tCTS with 2, 4, 6, 8, or 12-bp mm). Based on the PAM orientation, templates are referred to as PAM "In" (3′ of the crRNA sequence, red) or PAM "Out" (5′ of the crRNA sequence, blue). (B) Experimental setup to evaluate co-electroporation of RNPs and dsDNA donor templates with or without CTS motifs. (C) (Left) Schematics of transgene-encoded receptors and representative flow cytometry plots depicting editing outcomes using non-modified dsDNA HDRTs or with 4-bp mm PAM "In" or PAM "Out." (Right) Summary of flow cytometric analysis 4 days after electroporation ($n = 6$ for *CD3ε*-, $n = 3$ for *CD3ζ*-, and $n = 4$ for *TRAC*-knock-in into healthy donors). Black lines indicate mean values. HDR efficiencies and number of transgene-expressing cells are shown relative to the dsDNA condition in gray. For each knock-in condition, 0.5 μg template was used.

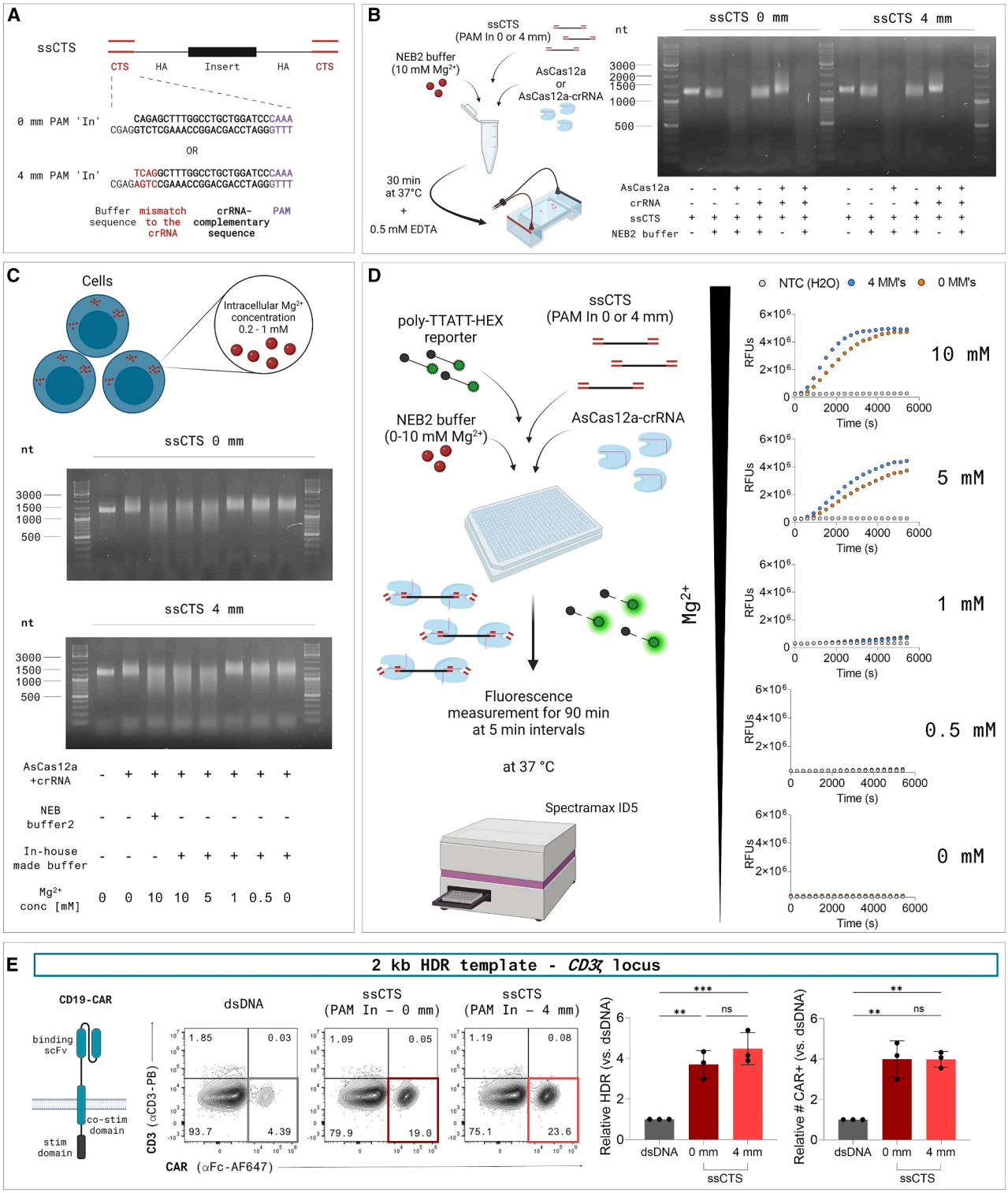


**Figure 2. Hybrid dsDNA modifications with Cas12a target sequence improve knock-in efficacy of linear ssDNA without triggering ssDNase activity of AsCas12a under physiological Mg2+concentrations**

(A) Designs of ssCTS donor templates are shown. The insert is flanked by HAs and hybridized CTS motifs. The CTS includes a 4-bp buffer region on the antisense strand, a PAM, and either an intact (CTS with 0-bp mismatch) or a truncated crRNA sequence (tCTS with 4-bp mismatches [mm]). (B) *In vitro* Cas12a cleavage assay depicting

*(legend continued on next page)*

AsCas12a. Given the high $Mg^{2+}$ level in the NEB2 buffer (10 mM), we hypothesized that no degradation of ssCTS would occur under lower $Mg^{2+}$ conditions that mimic physiological intracellular concentrations (0.2–1 mM). To test this, we co-incubated the HDRTs with the crRNA-nuclease complex in an in-house-prepared NEB2-like buffer containing a range of $Mg^{2+}$ concentrations. Comparable to the buffer-free condition, there was no evidence of nonspecific degradation of either intact or truncated ssCTS in the presence of the buffer containing low $Mg^{2+}$ concentrations (Figure 2C). To ensure the feasibility of proceeding with this nuclease in gene editing experiments, we decided to perform a more sensitive digestion assay[46] that detects *trans*-cleavage of ssDNA reporters as an indicator of AsCas12a collateral ssDNase activity (Figure 2D). To mimic an intracellular setting, we conducted this assay in buffers with varying $Mg^{2+}$ concentrations. As expected from the previous digestion assays, *trans*-cleavage activity was detected only when high $Mg^{2+}$ concentrations were used. When comparing the two ssCTS templates, there was no difference in the measured *trans*-cleavage under low $Mg^{2+}$ levels, as no digestion occurred.

After excluding an ssDNase activity of AsCas12a in $Mg^{2+}$-low environments, we proceeded to test the intact and 4-bp truncated ssCTS HDRTs in electroporation experiments using the same workflow as previously outlined (Figure 1B). The use of ssCTS templates led to a relative increase in knock-in rates by at least 3-fold (up to 5.5-fold). In contrast to previous experiments with dsCTS HDRTs (Figure 1), ssCTS also increased the absolute number of CAR-expressing cells relative to non-modified dsDNA (Figure 2E). When comparing intact versus truncated ssCTS, slightly higher HDR rates were observed when a 4-bp mm to the crRNA was included in the CTS motifs, but these differences were not statistically significant. These results suggest that both intact and truncated ssCTS can be utilized for efficient AsCas12a Ultra-mediated HDR, achieving significantly higher HDR rates and number of CAR-expressing cells compared to dsDNA templates.

### Incorporating a buffer region and introducing crRNA mismatches into the CTS region enhance gene editing outcome with AsCas12a

After confirming the efficacy of ssCTS as a template for CRISPR-Cas12a gene editing, we aimed to further optimize the CTS motifs for ssDNA. To this end, we evaluated the impact of different buffer sequences adjacent to the CTS (Figure S2A). We created ssCTS either with or without a 4-bp buffer sequence placed on the template strand alone (OS) or on both the template strand and the annealed ODN (TS) (Figure S2A). The inserted template for gene editing at the *CD3ζ* locus was the same 1.2-kb-sized CD19-CAR (2 kb including HAs) as used before (Figure 2E). When comparing ssCTS without a buffer sequence, there was no statistically significant difference in the non-modified ssDNA conditions (Figure S2B). In contrast, higher HDR frequencies were observed with the addition of an OS or TS-buffer, especially when using truncated templates. For instance, the transgene was detected in an average of 22% of T cells (± SD 8.25) when using OS ssCTS 2 mm and in 21% of T cells (± SD 8.76) with OS ssCTS 4 mm. Given the similar performance of these formats, we proceeded with OS 4 mm in the subsequent experiments.

### ssCTS donors outperform dsDNA templates at high concentrations independent of the transgene or insertion site

Following the selection of the most optimal CTS modification for CRISPR-Cas12a gene editing, we aimed to compare our ssCTS template with dsDNA, dsCTS, and ssDNA. The Cas12a-binding motifs of both ssCTS and dsCTS included a buffer sequence, a 4-bp mm to the crRNA, and a PAM "In" orientation (Figure 3A). To eliminate any bias specific to the construct or locus, we compared different concentrations of the various HDRT formats by insertion of an HLA-A2-TRuC into the *CD3ε* locus and CD19-CARs into *CD3ζ* or *TRAC* locus. In the case of the HLA-A2-TRuC (1.6 kb including HAs), the incorporation of CTS motifs increased HDR of dsCTS and ssCTS compared to dsDNA and ssDNA, respectively, across various concentrations (Figure 3B, top panel). However, with dsCTS, toxic doses were encountered starting at 50 nM, resulting in a progressive decline in knock-in efficiency and total cell yield. In contrast, ssCTS templates did not affect cell yield, even at the highest tested concentration (100 nM). Additionally, HDR frequencies increased with higher template concentrations without reaching a plateau. Notably, transgene expression was detected in up to 90% of T cells when using ssCTS at the highest HDRT concentration. When repeated independently in another laboratory using the same batch of ssCTS HDRT or a newly generated batch, HDR efficiencies were comparably high, reaching up to 92% (Figure S3). Similar trends were observed for *CD3ζ*-directed HDR insertion of a CD19-CAR, with ssCTS templates leading to transgene detection in up to 44% of T cells at the highest concentration (Figure 3B, middle panel). Lastly, non-viral gene editing was conducted using the larger

digestion of both intact and truncated ssCTS templates in 10 mM $Mg^{2+}$-containing NEB2 buffer after 30 min incubation at 37°C followed by reaction quenching with 0.5 mM EDTA. (C) *In vitro* Cas12a cleavage assay depicting digestion of both intact and truncated ssCTS templates in either 10 mM $Mg^{2+}$-containing NEB2 buffer or an in-house prepared buffer with various $Mg^{2+}$concentrations (absence, physiological intracellular conditions 0.2–1 mM, or excess 5–10 mM) after 30 min incubation at 37°C and reaction quenching with 0.5 mM EDTA. (D) Fluorescence-based CRISPR detection assay utilizing a poly-TTATT-HEX reporter was employed for detection of Cas12a-cleavage activity across varying $Mg^{2+}$-concentrations (0, 0.5, 1, 5, and 10 mM $Mg^{2+}$). Fluorescence measurements were acquired for 90 min at 5-min intervals using a multi-mode microplate reader (Spectramax iD5) with an excitation/emission wavelength pair of 530/570 nm. (E) (Left) Schematic of CD19-CAR receptor and representative flow cytometry plots depicting editing outcomes using dsDNA and intact or 4-bp mm ssCTS PAM "In". (Right) Summary of flow cytometric analyses 4 days after electroporation ($n = 3$ for *CD3ζ*-knock-in into healthy donors). Thick lines indicate mean values; error bars indicate standard deviation. Black dots represent individual data points. HDR efficiency and numbers of CAR-expressing cells are shown relative to the dsDNA condition in gray. For each knock-in condition, 0.5 μg template was used. Statistical analysis was performed using ordinary one-way ANOVA with subsequent Dunn's correction (for multiple testing) comparing values for each HDRT format with dsDNA as reference. Asterisks represent different $p$ values calculated in the respective statistical test (not significant [ns]: $p > 0.5$; $^{*}p < 0.05$; $^{**}p < 0.01$; $^{***}p < 0.001$).

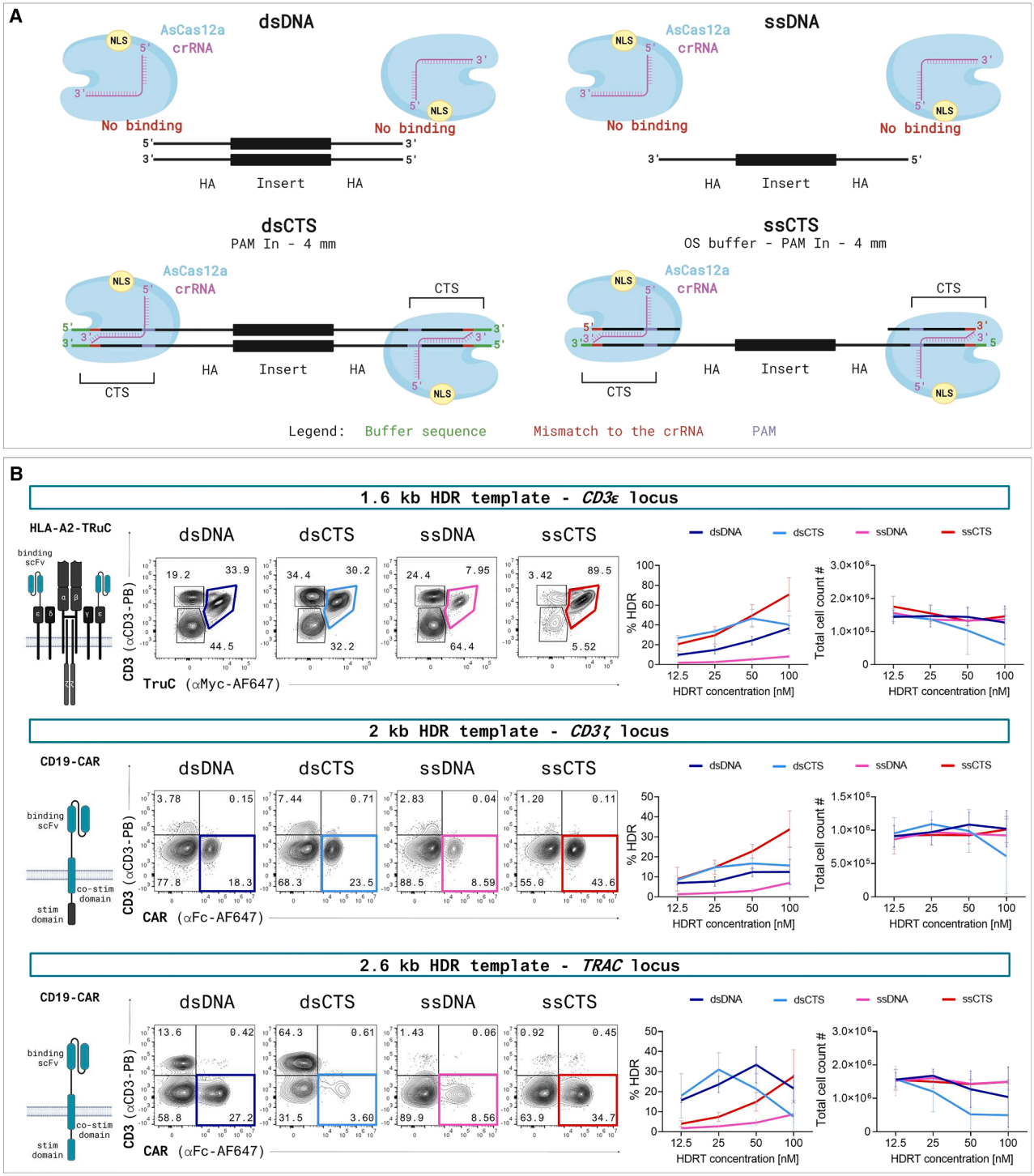


**Figure 3. Truncated CTS-modified ssDNA containing a buffer sequence and PAM "In" orientation outperform dsDNA templates at high concentrations**

Virus-free insertion of an HLA-A2-TRuC or two CD19-CAR transgenes into the human *TRAC*, *CD3ζ* or *CD3ε* loci. (A) Schematics of the interactions of the NLS-containing Cas12a-crRNA complex with the CTS motifs of dsDNA and ssDNA templates. Both CTS-containing construct formats contain CTS truncated by a 4-bp mm, have a PAM "In" orientation, and a buffer region. (B) (Left) Schematics of transgene-encoded receptors and representative flow cytometry plots depicting editing outcomes using dsDNA,

*(legend continued on next page)*

*TRAC*-CD19-CAR knock-in construct (2.6 kb including HAs) (Figure 3B, lower panel). Both dsDNA and dsCTS templates exhibited high frequencies of HDR at concentrations of 25 nM–50 nM but also showed a decrease in efficiency concomitant with a loss in cell numbers. In contrast, ssCTS showed a gradual increase in HDR, achieving transgene insertion frequencies ranging from 5% at 12.5 nM to 35% at 100 nM without a drop in cell numbers.

In summary, irrespective of the transgene or target locus, CTS motifs were essential additions to ssDNA templates to facilitate highly efficient CRISPR-Cas12a gene knock-in. With these end modifications, high concentrations of ssCTS consistently resulted in higher knock-in rates and improved cell yields compared to dsDNA and dsCTS.

### Small molecules that block non-homologous end-joining or microhomology-mediated end-joining do not increase ssCTS-mediated HDR of CAR transgenes

To investigate whether small molecules that modulate DNA repair pathways could enhance HDR efficiency with ssCTS templates, we tested a panel of compounds previously reported to improve HDR[28,34,47] (Figure S4). These included DNA-dependent protein kinase inhibitors (M3814 and AZD7648), the Alt-R HDR Enhancer V2, and DNA polymerase theta inhibitors (ART558 and Novobiocin), tested either individually or in specific combinations. Additionally, a TREX1 inhibitor was included based on reports that protecting ssODN donor templates from TREX1-mediated degradation can enhance HDR efficiency.[48] Consistent with prior studies, several of these small molecule treatments enhanced HDR efficiency when using dsDNA templates, with combinations such as AZD7648 + ART558 achieving up to a 2-fold increase compared to untreated controls (Figure S4). In contrast, ssCTS-edited cells showed no improvement in HDR efficiency in response to any of the tested enhancer conditions.

### CD19-CAR T cells generated with ssCTS donors display efficient cytotoxicity and expansion in co-cultures with tumor cells

To evaluate potential advantages of using ssCTS templates for therapeutic cell manufacturing, we assessed antigen-specific cytotoxicity and serial killing capacity of CD19-CAR-T cells (Figure S5). CD19-CARs were inserted into the *TRAC* locus using three HDRT formats (Figure S5A) —dsDNA, ssDNA, or ssCTS—and tested across a range of template doses (1 μg, 2 μg, and 4 μg). Short-term cytotoxicity of the different bulk-edited CAR T cells was evaluated with a VITAL assay, which quantifies the specific killing of CD19-positive target cells (Nalm6-CD19$^{WT}$) relative to CD19-negative controls (Nalm6-CD19$^{KO}$) (Figure S5B left). The ssCTS-edited T cells consistently demonstrated strong cytolytic activity, comparable to those edited with dsDNA that had similar CAR knock-in rates. In contrast, ssDNA-edited T cells exhibited reduced cytotoxicity across all conditions, particularly at a lower HDRT dose (Figure S5C). Next, a CAR-T cell rechallenge assay was performed to monitor expansion and serial killing capacity upon repeated tumor challenges. Engineered T cells were sequentially co-cultured with Nalm6-CD19$^{WT}$ GFP$^{+}$ target cells over four rounds at 2- to 3-day intervals (Figure S5B right). T cell proliferation was assessed, and functional persistence was evaluated by tracking the number of remaining GFP+ target cells over time. While dsDNA- and ssCTS-edited T cells showed sustained cytotoxic activity and robust expansion across all doses, ssDNA-edited T cells exhibited limited expansion and a decline in cytotoxicity over successive stimulations at lower HDRT doses (Figure S5C). Overall, short-term cytotoxicity and serial killing capacity correlated to the relative HDR rates determined by flow cytometry, with higher percentage of CAR-positive cells translating to higher tumor lysis. Notably, in conditions with higher HDRT doses (2 μg and 4 μg), both dsDNA- and ssCTS-edited T cells demonstrated increased expansion through the third stimulation, followed by a decline at the fourth stimulation. However, ssCTS-edited T cells showed higher expansion rates (up to 5.9-fold) compared to dsDNA-edited T cells (up to 4.8-fold) in these high-dose HDRT conditions.

### Long-read sequencing of on-target editing outcomes demonstrates efficient knock-in with ssCTS donors and less unintended integration events

Finally, we sought to investigate on-target gene editing outcomes of CD19-CAR T cells generated with dsDNA, ssDNA, or ssCTS. To this end, we performed PCR and long-read sequencing using Oxford Nanopore Technologies (ONT) to quantify the read length distributions (Figure 4). The primers were placed approximately 2 kb up- and downstream of the *TRAC* on-target site, resulting in a 4.3 kb amplicon read length for the unedited *TRAC* locus. The majority of reads in all groups were unedited or contained small indels, whereas a smaller proportion corresponded to perfect knock-ins, partial insertions, or longer reads (Figure 4A). Among the three template types, ssCTS-edited T cells exhibited the highest percentage of perfect knock-ins. Notably, a high frequency of partial knock-ins was observed across all donor types. When analyzing insertion events specifically (filtering on reads larger than 4.3 kb, Figure 4B), ssDNA-edited samples displayed nearly 80% partial knock-ins. Sub-analysis of the integration reads that contained the CAR gene demonstrated that partial integration events with ssDNA contained partial transgenes of variable length (Figure 4C). In contrast, ssCTS-edited cells had the lower level of partial insertions. Additionally, multi-template insertions that contained repeats of the homology arm sequences—likely representing homology-independent targeted integration through end-joining—were uniquely observed in dsDNA-edited cells, reaching 6.18% of reads filtered for integration events (exceeding 4.3 kb size) (Figure 4B). Overall, ssCTS donors

dsCTS, ssDNA, and ssCTS HDRTs. (Right) Summary of flow cytometric analyses 4 days after electroporation ($n$ = 3 for *CD3ε*-, $n$ = 4 for *CD3ζ*-, and $n$ = 3 for *TRAC*-knock-in into healthy donors, each from two independent experiments). Dark and light blue indicate the use of dsDNA and dsCTS templates, whereas pink and red depict ssDNA and ssCTS, respectively. Thick lines indicate mean values; error bars indicate standard deviation. The percentage of HDR efficiency and total cell numbers are shown in an HDRT concentration-dependent manner.

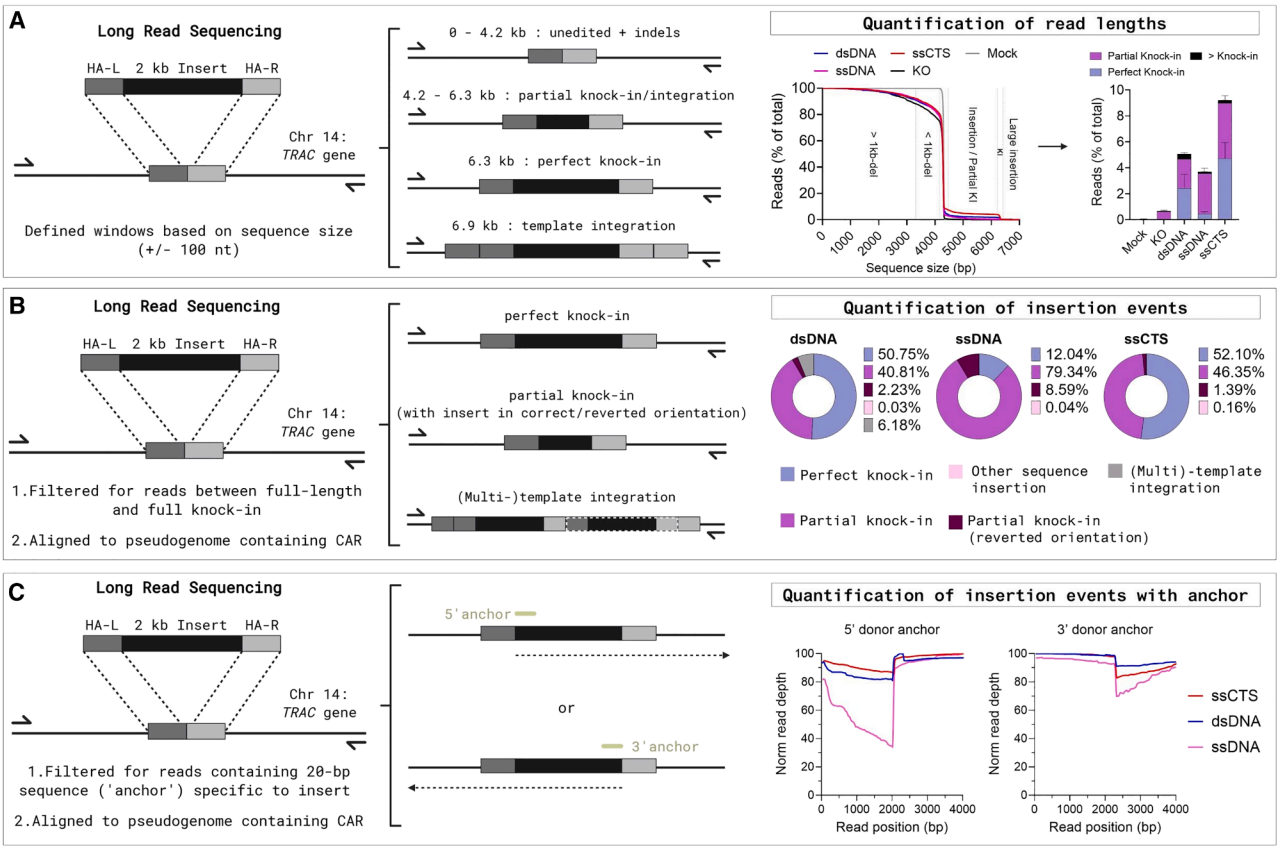


**Figure 4. Long-read sequencing reveals that ssCTS donors support efficient knock-in with high on-target integration fidelity**

(A) Schematic overview of the long-read sequencing strategy targeting the *TRAC* locus with primers placed ~2 kb upstream and downstream of the insertion site. Read length distributions were used to distinguish unedited alleles, partial knock-ins, perfect knock-ins, and extended integration events. Graphs on the right summarize the frequency of each read category across donor formats (dsDNA, ssCTS, and ssDNA). (B) Reads exceeding 4.3 kb in length were aligned to a pseudogenome containing the CD19-CAR transgene and categorized into distinct insertion types, including perfect and partial knock-ins (including reversed orientation) and multi-template integration events. Pie charts show the proportion of each event type per donor condition. (C) Insert-specific 5′ and 3′ anchor sequences were used to filter reads. Normalized read depth plots illustrate the continuity and distribution of integrated sequences across the three donor types.

yielded the highest HDR efficiency and lower levels of undesired insertional outcomes than unmodified linear ssDNA.

## DISCUSSION

The field of gene therapy has been rapidly progressing, marked by numerous ongoing clinical trials and extensive preclinical studies exploring innovative products.[49] CRISPR-Cas technology is gaining prominence due to its potential to tackle existing safety concerns and simplify the complex and costly manufacturing processes of gene therapy products, such as CAR-T cells.[3] However, further optimization is necessary to maximize the yield and improve the quality of gene-modified cells. One defining parameter determining the efficiency of gene editing is the donor template format. Despite the current scarcity of systematic studies comparing the design elements of synthetic templates, it has been established that ssDNA constructs are notably less harmful to cells.[15] Here, we demonstrated that the manufacture of genetically engineered T cells using CRISPR-Cas12a could be significantly improved by employing ssDNA templates with double-stranded CTS end modifications.

Our results suggest that incorporating CTS into linear ssDNA donor templates is a powerful tool to optimize gene transfer with different Cas species and in a non-viral fashion. We have independently replicated findings by Shy et al.[34] reporting that ssCTS templates significantly improve HDR efficiency with SpCas9-mediated gene editing in comparison to dsDNA or unmodified ssDNA. To translate the ssCTS approach to another Cas editing platform, we reasoned that optimization of CTS would be necessary to account for the differences in target interrogation between orthogonal Cas enzymes. This involved examining dsDNA containing both intact and truncated CTS sequences. Similar to previously reported CTS modifications for SpCas9,[24,34] PAM "In" orientation and low number of mismatches up to 4 bp at the 5′ end of the crRNA target sequence resulted in enhanced HDR efficiencies with the AsCas12a Ultra

enzyme. For SpCas9, truncated CTS was superior to CTS without mm. With AsCas12a, constructs with perfect CTS lacking any mismatches but containing a PAM 3′ of the crRNA (PAM "In") also outperformed non-modified donor templates. This may be attributed to the characteristic of Cas12a to cut distally from the PAM, thereby restricting the cleavage to the 5′ end of the template. Moreover, excessive mm to the crRNA target sequence led to a decrease in editing efficiency, likely due to the reported low intrinsic tolerance of AsCas12a for mismatches within regions proximal (1–18 bp) to the PAM.[40,50] These results increase the confidence that incorporation of CTS can be adapted to other Cas species, beyond SpCas9 and AsCas12a Ultra.

To utilize the AsCas12a nuclease for gene editing with ssCTS templates, we investigated its reported non-specific ssDNase activity as previously described.[44,45] Collateral Cas12a-mediated damage to ssDNA HDRTs after CTS-binding *in vitro* or induction of the DSB at the on-target locus would be detrimental to efficient gene editing. Our original hypothesis was that templates with double-stranded truncated CTS would be less susceptible to digestion compared to intact ones. However, cleavage of ssCTS templates occurred only under conditions with non-physiologically high concentrations of $Mg^{2+}$, confirming previous findings.[44] Considering that magnesium is the fourth most abundant positively charged ion in the body and the second most abundant within cells,[51] this raised questions about how intracellular magnesium levels might influence the nonspecific cleavage of ssCTS by AsCas12a. As the concentration of free magnesium inside cells varies between 0.5 and 1 mM,[52] we aimed to investigate ssDNase activity under physiological $Mg^{2+}$ concentrations. By measuring *cis*- or *trans*-cleavage under varying $Mg^{2+}$ concentrations and testing the nuclease with our templates from electroporation experiments, our findings indicated that AsCas12a does not induce excessive ssDNA degradation. Consequently, no discernible difference was observed between the intact and truncated CTS constructs. Our results suggest that there is no overt ssDNase activity of AsCas12a Ultra in human T cells. Others have previously reported that ssDNase activity of Cas12a systems did not contribute to bacterial host defense against bacteriophages,[53] suggesting that the ssDNase phenomenon could be primarily restricted to *in vitro* settings. Moreover, one study demonstrated that *in vitro* collateral ssDNase activity is less pronounced in AsCas12a than in other Cas12a enzymes such as LbCas12a.[54]

The ssCTS templates enabled efficient gene transfer of various clinically relevant, intermediate-sized transgenes, but with notable template-size dependent variabilities. The ssCTS templates outperformed dsCTS HDRTs in terms of both cell viability and HDR efficacy at the highest concentration tested. In general, notable differences were observed in the transgene insertion efficiency between larger and smaller constructs. For instance, using a 0.8-kb-sized insert into the *CD3ε* gene led to the detection of the transgene in up to 90% of the cells, whereas only 35% of the cells expressed a 1.8-kb-sized insert at the *TRAC* locus. Although these differences might also be locus-dependent, the observed association between size and toxicity is consistent with previous findings with the SpCas9-ssCTS platform,[34] suggesting that larger HDRTs tend to induce greater toxicity in cells. This toxic effect was considerably more pronounced in dsDNA templates compared to ssCTS. The exact reason for the reduced toxicity of ssCTS relative to dsDNA in cellular systems is not yet fully elucidated, but it may be attributed to differential recognition by DNA-sensing pathways[55,56] or to increased physical stress by the larger dsDNA-RNP aggregates. Potentially, reduced toxicity by ssCTS templates could explain improved expansion capacity, which we observed *in vitro* (Figure S5). In our experiments, we did not reach a concentration at which ssCTS templates induced dose-dependent toxicity. As a next step, investigating higher concentrations of larger-sized ssCTS would be valuable to determine the highest potential knock-in rate for larger constructs. However, the production of highly concentrated and pure linear ssDNA remains a limitation to execute these suggested experiments. In our hands, linear ssDNA HDRTs production by single-strand exonuclease digestion of dsDNA (see methods) becomes inefficient for constructs larger than 3kb. Other methods include biotin-streptavidin bead selection of a labeled DNA strand[34,57] or asymmetric PCR,[58] but they suffer from reduced purity. Alternatively, commercial providers previously manufactured high-quality linear ssDNA at high concentration for dose-escalation studies with larger ssCTS HDRTs,[34] and others have demonstrated that circular ssDNA produced from phagemids is suitable for large-scale production of large HDRTs, up to 13 kb in size.[59] Future studies may investigate whether knock-in efficacy of circular ssDNA HDRTs can be increased with CTS. Interestingly, in contrast to dsDNA donors, the addition of small-molecule HDR enhancers—such as DNA-PK inhibitors or Polθ inhibitors—did not increase knock-in efficiency with long linear ssDNA templates containing moderately sized transgenes, suggesting that ssDNA-mediated HDR may proceed through distinct pathways (Figure S4).[60]

To our knowledge, this is the first study comparing the integration outcomes in T cells using different long linear ss/dsDNA template formats by long-read sequencing. While the results corroborated relative knock-in efficiencies for perfect CAR integrations as measured by flow cytometry, long-read data additionally enabled the assessment of undesired integration events at the on-target locus. Hybridizing oligos that create dsDNA CTS end modifications in ssCTS donors reduced the relative frequency of partial integration events observed with linear ssDNA (Figure 4). The high frequency of partial integration events observed with linear ssDNA might be related to suboptimal donor quality and/or trimming of the ssDNA ends by cellular exonucleases, such as TREX1.[48] Of note, we detected events containing transgenes in the reverse orientation, especially in conditions treated with linear unmodified ssDNA templates. Future studies may decipher the underlying repair mechanism of undesired events and devise strategies to avoid them. Partial integration events could potentially be reduced by preventing exonuclease damage by chemical modifications[48,61] or pharmacological inhibition of exonucleases.[48]

The experiments with ssCTS with SpCas9[34] and AsCas12a (this study) demonstrate that insufficient nuclear delivery after electroporation of non-viral ssDNA templates likely impedes efficient editing. Alternative strategies to increase nuclear concentration of ssDNA HDRTs involve other means of coupling the DNA donors with the NLS-tagged gene editor directly, creating a tripartite complex of NLS-SpCas9 with sgRNA and circular ssDNA templates.[62] Future studies may elucidate other means to deliver ssDNA templates for efficient, non-toxic editing and explore different transfection modalities, such as lipid nanoparticles or chemical transfectants, with and without peptide-mediated Cas delivery.[63,64]

Altogether, by incorporating CTS to overcome the nuclear transport barrier and by leveraging the decreased cellular toxicity of ssDNA, ssCTS constructs provide a compelling alternative to dsDNA-mediated HDR in non-viral CRISPR-Cas12a gene editing. For smaller transgenes, such as CD3ε-TRuC used in our study, ssCTS templates can reach integration rates as high as 90%. These efficiencies mirror integration frequencies previously only achieved with recombinant adeno-associated virus for template delivery.[65] Moreover, ssCTS templates offer a promising solution to the hurdle of obtaining sufficient numbers of transgene-positive cells without the need for additional purification steps,[18] pharmacological enhancers,[28,34] or knock-in into essential genes[66] since higher donor concentrations can be used without causing relevant toxicity. Clinical translation of ssCTS repair templates will require sourcing of the materials from appropriate manufacturers to ensure quality sufficient for clinical testing (e.g., low degree of impurities and high sequence fidelity). Warranting successful scale-up and extended genotoxicity studies, the AsCas12a-ssCTS platform could improve the virus-free manufacturing process for adoptive T-cell-based therapies for future clinical applications.

## MATERIALS AND METHODS

### PBMC isolation and T cell enrichment

The research was conducted in accordance with the Declaration of Helsinki. Peripheral blood samples were collected from consenting healthy adult individuals under the approval of the Charité ethics committee (approval code EA1/052/22). Peripheral blood mononuclear cells (PBMCs) were isolated through density-gradient centrifugation. For this, 50-mL LeucoSEP tubes (Greiner Bio-One GmbH) were used, to which 15 mL of BioColl separating solution (Ficoll) (Bio&SELL GmbH) was added per tube. The tubes were then quickly spun down, in order for the solution to pass the porous filter. Fresh heparinized whole blood was mixed in a 1:1 ratio with sterile phosphate-buffered saline (PBS) (Gibco) and poured into the Ficoll-containing tubes. Centrifugation was carried out at 1,000 × g for 20 min employing minimal break speed (acceleration 6 and deceleration 3). The mononuclear cell layer was then collected, diluted in sterile PBS, and subjected to two centrifugation steps with break at 300 × g for 10 min, each with subsequent removal of the supernatant. Afterward, the PBMC pellet was resuspended in 50 mL of PBS and counted using the CASY cell counter (OMNI Life Science GmbH & Co. KG). Finally, PBMCs were positively enriched for CD3+ T cells using magnetic column enrichment with human CD3 microbeads, following the manufacturer's recommendations (LS columns, Miltenyi Biotec, Germany).

### Cell culture

T cells were cultured in 44.5% Click' medium (Irvine Scientific) and 44.5% Advanced RPMI medium 1640 (Gibco), including 10% heat-inactivated fetal calf serum (FCS) (Sigma-Aldrich), 1% GlutaMAX (100X) (Gibco), recombinant interleukin-7 (IL-7) (10 ng/mL), and IL-15 (5 ng/mL) (CellGenix GmbH). T cell activation was carried out for 48 h on tissue culture plates coated with anti-CD3/28 antibodies. For this, 24-well-tissue-culture plates (Corning) were incubated overnight at 4°C with 500 µL/well of sterile ddH2O supplemented with 1 µg/mL anti-CD3 monoclonal antibody (mAb) (clone OKT3; Invitrogen) and 1 µg/mL anti-CD28 mAb (clone CD28.2; BioLegend). Afterward, the plates were rinsed twice in PBS and once in RPMI without allowing the wells to dry. T cells were then seeded at a density of 1–1.5 × $10^6$ cells per well and cultured at 37°C, 5% $CO_2$.

### Design of plasmids encoding homology-directed repair templates

The majority of DNA templates used in this study were generated from previously published plasmids.[5,28,67] These encoded receptors or fusion constructs, such as CD19-CARs and HLA-A2-TRuC, intended for integration into specific loci of primary human T cells, including the *T cell receptor α constant chain* (*TRAC*), *CD3ζ* (*zeta chain of the CD3 complex*), or *CD3ε* (*epsilon chain of the CD3 complex*). Both the CAR and TRuC constructs were flanked by approximately 400-bp-long HAs complementary to the genomic DNA sequence next to the cutting site of interest as previously described.[5,23,28,67] For the *TRAC*-directed CAR templates, a second-generation CAR design was employed. This included a CD19-binding single-chain variable fragment (scFv) with an immunoglobulin G1 (IgG1) hinge region followed by a CD28 transmembrane and co-stimulatory region and a CD3ζ domain. The heavy chain of the scFv was connected to the light chain via a triple glycine and 4 serine-rich (3xG4S) linker. In the case of the *CD3ζ*-directed CARs, no exogenous stimulatory CD3ζ was integrated into the design, as the endogenous CD3ζ is recruited for CAR assembly.[5] All CAR constructs featured a porcine teschovirus-1 2A (P2A) sequence positioned upstream of the scFv domain and following this, a membrane leader sequence. The *TRAC* construct also included a bovine-growth-hormone-derived polyadenylation site (bGH poly A). No poly A was added to the *CD3ζ*-directed templates because the CAR transgene was inserted in-frame into the gene encoding the CD3ζ protein.[5] Of the two *CD3ζ*-directed CARs used, one contained a Myc-tag. In contrast to the CARs, the TRuC template was composed solely of a Myc-tag, an HLA-A2-binding scFv, and two 3xG4S linkers—one for linking the light and heavy chains of the antibody fragments and one for binding the endogenous CD3ε chain. All plasmid sequences are listed in Table S1; the original *CD3ζ*-HDRT and the original *TRAC*-HDRT are available via Addgene (CD3ζ -truncCARgsg: Addgene ID 215759, TRAC-Cas12a: 215769).

### In-fusion cloning strategy of plasmids

The cloning of plasmids encoding HDRTs was conducted using the two-fragment In-Fusion method following the manufacturer's protocol (Clontech, Takara Bio). For the *CD3ζ*-directed CD19-CAR construct containing a Myc-tag, an In-Fusion cloning strategy was planned with SnapGene (from Insightful Science; snapgene.com). The CAR transgene and the backbone were PCR amplified from previously published plasmids,[5,67] and the resulting products were purified using the DNA Clean and Concentrator-5 Kit following the manufacturer's instructions (Zymo Research). In-Fusion reactions were prepared in 5 μL volumes at a 1:3 vector to insert molar ratio. Subsequently, 2.5 μL of the In-Fusion reaction mixture was transformed into Stellar Competent *E. coli* (Takara Bio) in 10 μL reactions and then plated on LB (Carl Roth GmbH) broth agar plates supplemented with ampicillin (Sigma-Aldrich). Following colony PCR for size validation, preferred clones were cultured overnight at 37°C, 200 rpm in 3–5 mL ampicillin-containing bacterial cultures. Plasmids were purified using the ZymoPURE Plasmid Mini Prep Kit (Zymo Research). Lastly, sequence confirmation of HDR donor-template-containing plasmids was accomplished through Sanger Sequencing (LGC Genomics, Berlin).

### Primer and oligo design for CTS HDR templates

Primers for generating HDR templates with various CTS motifs were designed as recently described[24,34] and synthesized by IDT. In the case of dsCTS, all primers were composed of a 16-bp-long buffer sequence, the specific gRNA or crRNA target sequence with mismatches ranging from 0 to 12 bp, a PAM, and the complementary sequence for amplification. A similar design was employed for generating ssCTS, except for the use of either a shorter 4-bp-long buffer sequence or no buffer sequence at all. Moreover, primers for ssDNA production were either 5′ or 3′ phosphorylated. For the generation of ssCTS templates with double-stranded ends, complementary oligos were designed and synthesized by IDT. All oligos included the specific guide RNA target sequence with 0, 2, 4, or 6 bp mismatch, the PAM, and the complementary sequence to the homology arms. Only some oligos contained a buffer sequence. All primer and oligo sequences are listed in Table S2.

### Generation of double-stranded and single-stranded DNA for homology-directed insertion of receptors

The HDR templates were amplified from plasmids by PCR using the KAPA HiFi HotStart 2× Readymix (Roche) with reaction volumes of either 500 μL or 1,000 μL. The resulting dsDNA amplicons were concentrated and purified using paramagnetic beads (AMPure XP, Beckman Coulter Genomics). In this process, PCR products were mixed with the beads in a 1:1 ratio, incubated at room temperature for 10 min, and then placed in a DynaMag-2 stand (Invitrogen, Thermo Fisher Scientific) for another 10 min. The bead-nucleic acid mix was washed two times under sterile conditions with freshly prepared 70% ethanol while still on the magnet. Finally, the DNA was eluted in 3 μL of nuclease-free water per 100 μL PCR product. The concentration of the nucleic acid was determined using either the Nanodrop ND-1000 spectrophotometer (Thermo Fisher Scientific) or the Qubit 2.0 fluorometer (Invitrogen, Life Technologies). For the generation of ssDNA templates via enzymatic digestion, the "Guide-it Long ssDNA Production System v2" kit was used according to the manufacturer's instructions (Takara Bio). In this process, the PCR products amplified with one phosphorylated primer were used. After ssDNA production, templates were purified and concentrated similar to the dsDNA cleanup, using AMPure XP beads. For the generation of double-stranded CTS ends on the ssDNA, complementary oligos were added at a 6:1 M ratio of oligos to nucleic acid. For the annealing, the mixed solutions were incubated at 94°C for 2 min, followed by 70°C for 1 min, and finally room temperature for 15 min. The concentration of all DNA templates was adjusted according to the knock-in experimental setup planned (range of 0.5–4 μg/μL).

### Ribonucleoprotein formulation and mix with DNA templates

Prior to the electroporation, RNPs were formed by mixture and incubation of 0.5 μL poly-L-glutamic acid (PGA) (Sigma-Aldrich, 100 mg/mL), 0.48 μL of crRNA or sgRNA (synthesized by IDT, 100 μM), and 0.4 μL of Alt-R AsCas12a (Cpf1) Ultra (synthesized by IDT, 64 μM) or Alt-R S.p. Cas9 Nuclease V3 (synthesized by IDT, 61 μM) for 15 min at room temperature. After the incubation, the RNPs were placed on ice until further use. For the electroporation of T cells with HDRTs containing CTS motifs, the DNA was pre-incubated for 5–10 min with the RNPs. Depending on the experimental setup, different HDRT amounts were used as indicated. Information regarding the crRNA or sgRNA target sequences can be found in Table S3.

### Electroporation

Non-viral knock-ins in T cells were performed as recently described.[28] Forty-eight-hour-stimulated primary T cells were harvested, counted, and washed twice in sterile PBS for 10 min, first at 150 × g and then at 100 × g. Afterward, $1 \times 10^6$ cells were resuspended in 20 μL P3-buffer (Lonza) per electroporation reaction and added to the RNP-HDRT mix. The suspension was carefully transferred to a 16-strip electroporation cuvette, which was then tapped on the bench repeatedly to guarantee proper positioning of fluids within the strip and the absence of bubbles that would interfere with the electric current. The cells were electroporated with the 4D-Nucleofector device (Lonza) using the program EH-115 according to previous reports.[23,28] Quickly after, 90 μL of pre-warmed medium was added per electroporation reaction, and the strip was incubated for 10 min at 37°C. Lastly, the cells were seeded to a 96-well round-bottom plate (50 μL cells/well) containing 150 μL pre-warmed T cell medium per well (with or without HDR-enhancing supplements) at a density of $0.5 \times 10^6$ cells per well. Small molecules were purchased from different commercial sources as dry powders solubilized in DMSO as directed. These included HDR enhancer V.2 (IDT), AZD-7648 (MedChemExpress), M3814 (MedChemExpress), Novobiocin (MedChemExpress), ART558 (MedChemExpress), and TREX1-IN-1 (MedChemExpress). Approximately 4 h after electroporation, 100 μL of the medium was exchanged in the conditions containing HDR-enhancing supplements.

### Flow cytometry

Gene editing read-outs were carried out via flow cytometry on 96-well round-bottom plates using a CytoFLEX LX device (Beckman Coulter). In order to allow ample protein turnover and ensure the visualization of transgene expression, cell counting and assessment of knock-in efficiency were performed at 4 and 7 days following electroporation. All staining panels are specified in Table S4. Cell concentrations were assessed by acquiring 30 µL of resuspended cells diluted 1:5 in PBS-4′,6-diamidino-2-phenylindole (DAPI) (Thermo Fisher Scientific) without any prior washing steps. For detection of transgene expression, a series of consecutive washing and staining steps were performed. A volume of 40–100 µL of cell suspension was transferred to a 96-well round-bottom plate and rinsed with 100–160 µL of PBS at 400 × g for 5 min. Subsequently, the supernatant was removed, and the cell pellets were briefly vortexed. For cells electroporated with HDRTs lacking a Myc tag, an initial surface stain was done using an anti-Fc antibody (αFc) (polyclonal, Jackson Immuno Research) conjugated to an Alexa Fluor 647 (AF647) fluorochrome. To achieve this, 30 µL of diluted αFc were added per staining condition, followed by incubation of cells at 4°C in the dark for 15 min. Afterward, the cells were washed again and stained a second time with a Pacific-Blue-conjugated anti-CD3 antibody (clone UCHT1, Biolegend) and a LIVE/DEAD-UV dye (Thermo Fisher Scientific). As for the cells electroporated with HDRTs containing a Myc tag, CAR detection was achieved with one staining using an anti-Myc antibody (clone 9B11, Cell Signaling Technology) coupled to AF647 and the same anti-CD3 antibody and LIVE/DEAD-UV dye mentioned before.

### *In vitro* AsCas12a cleavage assay with gel electrophoresis readout

Standard *in vitro* cleavage reactions were conducted using either commercially purchased NEB2 buffer (New England Biolabs) or an in-house-made version composed of 50 mM NaCl, 10 mM Tris-HCl (pH 7.9), and 100 µg/µL BSA, with varying concentrations of $MgCl_2$ (ranging from 0 to 10 mM). All reactions, containing either buffer were quenched by the addition of 8-fold molar excess of EDTA (0.5 M, Thermo Fisher Scientific) relative to the highest $Mg^{2+}$ concentration and then loaded on an agarose gel for assessment of ssDNA cleavage. In the assay, 0.5 µL of ssCTS substrates (0.25 µg per condition) were incubated at 37°C for 30 min, with different reagents depending on the condition tested. AsCas12a (64 µM) and crRNA (100 µM) were diluted 1:10 in nuclease-free water, and volumes corresponding to those from the electroporation were utilized (0.48 µL crRNA and 0.4 µL AsCas12a). All reactions were carried out in a total volume of 5 µL (excluding the EDTA used for reaction quenching), with nuclease-free water added as necessary to achieve this volume.

### Fluorescence-based CRISPR detection assay

Synthetic DNA was detected in a 20 µL CRISPR reaction in a 384-well microplate at 37°C.[46] CRISPR detection was performed with final concentrations of 250 nM poly-TTATT-HEX reporter; 90 nM AsCas12a; 45 nM crRNA; 50 mM NaCl; 10 mM Tris-HCl; 100 µg/mL BSA; and either 0, 0.5, 1, 5, or 10 mM $MgCl_2$. Fluorescence was measured on a multi-mode microplate reader (iD5) with an excitation/emission wavelength pair of 530/570 nm. Fluorescence measurements were read for 90 min at 5-min intervals.

### VITAL assay

Effector T cells (CD19-CAR T cells generated with dsDNA, ssDNA, or ssCTS) were co-cultured with target cells (Nalm-6 $CD19^{WT}$ GFP+ cells) and control cells (Nalm-6 CD19 $CD19^{KO}$ RFP+ cells) at various effector:target:control (E:T:C) ratios: 8:1:1, 4:1:1, 2:1:1, 1:1:1, 0.5:1:1, and 0.125:1:1. A suspension of 25,000 target and 25,000 control cells per well was prepared and added to the effector cells in 96-well, round-bottom plates. The plates were centrifuged at 100 × g for 3 min at room temperature, then incubated for 6 h at 37°C with 5% $CO_2$. After incubation, the cells were mixed, and 50 µL of the cell suspension was transferred to a prepared PBS-DAPI plate for flow cytometric analysis of GFP, RFP, and DAPI signals. Effector-cell-mediated cytotoxicity was calculated from shifts in the target:control cell ratio relative to control conditions without effector cells. The experiment was performed on day 12 after electroporation.

### CD19-CAR T cell rechallenge assay

Engineered CD19-CAR T cells were seeded into a flat-bottom, 96-well plate in RPMI 1640 (no phenol red) medium (Gibco) supplemented with 10% FCS. Twenty thousand GFP+ Nalm6-$CD19^{WT}$ target cells were given to the CAR T cells in a 5:1 tumor:CAR T cell ratio. The CAR T cells were sequentially stimulated with target cells every 2–3 days. T cell proliferation was assessed by transferring 50 µL of the cell samples to a PBS-DAPI plate for flow cytometry analysis, and functional T cell persistence was monitored by live cell imaging of GFP+ target cells over time using an IncuCyte device (Sartorius).

### Long-read sequencing

The following steps were carried out in an amplicon-free pre-PCR area; 500 ng of genomic DNA was amplified using NEBNext Ultra II Q5 HiFi polymerase (New England Biolabs) with primers containing stubbers for downstream indexing (TRAC_ONT_F: 5′-TTTCTGTTGGTGCTGATATTGCTTCAATCACTGCTGTGTCCCT-3’; TRAC_ONT_R: 5′-ACTTGCCTGTCGCTCTATCTTCTCCCACCCCAGACCTCCTAGTT-3′). The expected amplicon length was 4.3 kb surrounding the cut site. The following PCR cycle conditions were used: denaturation at 98°C for 30 s followed by 25 cycles of 98°C for 10 s, 60°C for 30 s, and 72°C for 10 min. PCR products were purified with 0.8X SPRI beads and eluted in $H_2O$. Libraries were indexed and generated using the PCR Barcoding Expansion 1–96 [EXP-PBC096] for Ligation Sequencing Kit [SQK-LSK114] (Oxford Nanopore). Purified libraries were sequenced on a PromethION with the R10.4.1 flow cell. Reads lengths were quantified using SummarizeOntDels (https://github.com/cornlab/summarizeOntDeletions).[68]

### Data analysis, statistics, and presentation

Flow cytometry data were analyzed using FlowJo software version 10 (BD Biosciences). Data from various assays were organized in Excel (Microsoft), and graphs were generated using Prism 9 (GraphPad). The impact of various template formats on gene editing efficacy was assessed through either one-way or two-way repeated measures ANOVA, followed by a Dunn's correction for multiple comparisons ($p < 0.05$). Diagrams depicting nucleic acid sequences, receptors, and experimental workflows in the figures were generated using www.biorender.com.

## DATA AVAILABILITY

All construct sequences can be found in Table S1. The CTS designs and corresponding DNA oligo sequences can be found in Table S2. The plasmids encoding the original *CD3ζ*-HDRT and the *TRAC*-HDRT are available via Addgene (CD3ζ-truncCARgsg: Addgene ID 215759, TRAC-Cas12a: 215769). The raw sequencing data underlying Figure 4 was deposited in the NCBI Sequence Read Archive (SRA) under the accession number: PRJNA1257358 (https://www.ncbi.nlm.nih.gov/bioproject/PRJNA1257358). All other data can be requested from the corresponding author upon request.

## ACKNOWLEDGMENTS

The authors would like to thank Tatiana Zittel (Charité) for her technical assistance. A.M.N., J.K., and D.L.W. would like to thank their direct support by the Jonas Center for Cellular Therapy of the University of Chicago, USA. This project has received funding from the European Union under Grant Agreement Nr. 101057438 (geneTIGA: genetiga-horizon.eu) to R.O.B., J.E.C., and D.L.W. Views and opinions expressed are however those of the author(s) only and do not necessarily reflect those of the European Union or the European Health and Digital Executive Agency (HADEA). Neither the European Union nor the granting authority can be held responsible for them. J.K. and D.L.W. were supported by the SPARK-BIH program by the Berlin Institute of Health, Germany. M.M.K. was supported by the Emmy Noether Programme (grant no. KA5060/1-1) of the German Research Foundation and is a participant in the BIH Charité Clinician Scientist Program funded by the Charité – Universitätsmedizin Berlin and the Berlin Institute of Health at Charité (BIH). J.E.C. is supported by the NOMIS Foundation, the Lotte und Adolf Hotz-Sprenger Stiftung, the Swiss National Science Foundation (project grants 310030_188858, 320030-227979, and 310030_201160), and the European Research Council (ERC) under the European Union's Horizon 2020 research and innovation program (grant agreement No 855741, DDREAMM).

## AUTHOR CONTRIBUTIONS

A.M.N. planned and performed experiments, analyzed results, interpreted the data, and wrote the manuscript. W.D. and V.G. designed the first CTS-templates for AsCas12a editing, planned and performed experiments, analyzed results, interpreted the data, and edited the manuscript. J.K. performed experiments, advised on the figures, interpreted data, and edited the manuscript. M.S. performed experiments and analyzed results. R.G. and M.K. planned, performed, analyzed, and interpreted data from *trans*-cleavage assay. N.S.M. and R.O.B. planned, performed, and interpreted replication studies with ssCTS. M.K. and R.O.B. provided reagents. E.J.A., G.C., and J.E.C. planned, performed, and interpreted the long-read sequencing results and edited the manuscript. D.L.W. designed and led the study, planned experiments, interpreted data, drafted figures, and edited the manuscript. All authors reviewed, commented, and approved the manuscript in its final form.

## DECLARATION OF INTERESTS

J.K., W.D., and D.L.W. are listed as inventors on patent applications on genome editing strategies to create CAR-redirected immune cells described in the manuscript (CD3-zeta editing: EP4019538A1—D.L.W. and J.K.; CD3-epsilon editing: EP4353252A1—D.L.W., J.K., and W.D.). D.L.W. is a co-founder of the startup TCBalance Biopharmaceuticals GmbH focused on regulatory T cell therapy. R.O.B. is a cofounder, equity holder, and consultant of UNIKUM Tx, holds equity in Kamau Therapeutics, reports research funding from Novo Nordisk, and is inventor of patents and patent applications related to CRISPR/Cas gene editing and cellular immunotherapies. None of these companies were involved in the present study. All other co-authors report no conflict of interest related to this work. J.E.C. is a co-founder and SAB member of Serac Biosciences and an SAB member of Relation Therapeutics, Hornet Bio, and Kano Therapeutics. The lab of J.E.C. has had funded collaborations with Allogene, Cimeio, and Serac.

## SUPPLEMENTAL INFORMATION

Supplemental information can be found online at https://doi.org/10.1016/j.omtn.2025.102568.

## REFERENCES

1. Bishop, M.R., Dickinson, M., Purtill, D., Barba, P., Santoro, A., Hamad, N., Kato, K., Sureda, A., Greil, R., Thieblemont, C., et al. (2022). Second-Line Tisagenlecleucel or Standard Care in Aggressive B-Cell Lymphoma. N. Engl. J. Med. Overseas. Ed. *386*, 629–639.
2. Westin, J., and Sehn, L.H. (2022). CAR T cells as a second-line therapy for large B-cell lymphoma: a paradigm shift? Blood *139*, 2737–2746.
3. Wagner, D.L., Koehl, U., Chmielewski, M., Scheid, C., and Stripecke, R. (2022). Review: Sustainable Clinical Development of CAR-T Cells – Switching From Viral Transduction Towards CRISPR-Cas Gene Editing. Front. Immunol. *13*.
4. Micklethwaite, K.P., Gowrishankar, K., Gloss, B.S., Li, Z., Street, J.A., Moezzi, L., Mach, M.A., Sutrave, G., Clancy, L.E., Bishop, D.C., et al. (2021). Investigation of product-derived lymphoma following infusion of piggyBac-modified CD19 chimeric antigen receptor T cells. Blood *138*, 1391–1405.
5. Kath, J., Franke, C., Drosdek, V., Du, W., Glaser, V., Fuster-Garcia, C., Stein, M., Zittel, T., Schulenberg, S., Porter, C.E., et al. (2024). Integration of ζ-deficient CARs into the CD3ζ gene conveys potent cytotoxicity in T and NK cells. Blood *143*, 2599–2611.
6. Song, P., Zhang, Q., Xu, Z., Shi, Y., Jing, R., and Luo, D. (2024). CRISPR/Cas-based CAR-T cells: production and application. Biomark. Res. *12*, 54.
7. Eyquem, J., Mansilla-Soto, J., Giavridis, T., van der Stegen, S.J.C., Hamieh, M., Cunanan, K.M., Odak, A., Gönen, M., and Sadelain, M. (2017). Targeting a CAR to the TRAC locus with CRISPR/Cas9 enhances tumour rejection. Nature *543*, 113–117.
8. Park, J.H., Palomba, M.L., Perica, K., Devlin, S.M., Shah, G., Dahi, P.B., Lin, R.J., Salles, G., Scordo, M., Nath, K., et al. (2025). Results From First-in-Human Phase I Study of a Novel CD19-1XX Chimeric Antigen Receptor With Calibrated Signaling in Large B-Cell Lymphoma. J. Clin. Oncol. JCO2402424. https://doi.org/10.1200/JCO-24-02424.
9. Lah, S., Kim, S., Kang, I., Kim, H., Hupperetz, C., Jung, H., Choi, H.R., Lee, Y.-H., Jang, H.-K., Bae, S., and Kim, C.H. (2023). Engineering second-generation TCR-T cells by site-specific integration of TRAF-binding motifs into the CD247 locus. J. Immunother. Cancer *11*, e005519.
10. Baeuerle, P.A., Ding, J., Patel, E., Thorausch, N., Horton, H., Gierut, J., Scarfo, I., Choudhary, R., Kiner, O., Krishnamurthy, J., et al. (2019). Synthetic TRuC receptors engaging the complete T cell receptor for potent anti-tumor response. Nat. Commun. *10*, 2087.
11. Shu, R., Hammett, M., Evtimov, V., Pupovac, A., Nguyen, N.-Y., Islam, R., Zhuang, J., Lee, S., Kang, T.H., Lee, K., et al. (2023). Engineering T cell receptor fusion proteins using nonviral CRISPR/Cas9 genome editing for cancer immunotherapy. Bioeng. Transl. Med. *8*, e10571.
12. Manske, K., Dreßler, L., Fräßle, S.P., Effenberger, M., Tschulik, C., Cletiu, V., Benke, E., Wagner, M., Schober, K., Müller, T.R., et al. (2024). Miniaturized CAR knocked onto CD3ε extends TCR function with CAR specificity under control of endogenous TCR signaling cascade. J. Immunol. Methods *526*, 113617.
13. Du, W., Noyan, F., McCallion, O., Drosdek, V., Kath, J., Glaser, V., Fuster-Garcia, C., Yang, M., Stein, M., Franke, C., et al. (2025). Gene editing of CD3 epsilon to redirect regulatory T cells for adoptive T cell transfer. Mol. Ther. *33*, 997–1013.
14. Muller, Y.D., Ferreira, L.M.R., Ronin, E., Ho, P., Nguyen, V., Faleo, G., Zhou, Y., Lee, K., Leung, K.K., Skartsis, N., et al. (2021). Precision Engineering of an Anti-HLA-A2 Chimeric Antigen Receptor in Regulatory T Cells for Transplant Immune Tolerance. Front. Immunol. *12*, 686439.
15. Shakirova, A., Karpov, T., Komarova, Y., and Lepik, K. (2023). In search of an ideal template for therapeutic genome editing: A review of current developments for structure optimization. Front. Genome *5*, 1068637.

16. Horlbeck, M.A., Witkowsky, L.B., Guglielmi, B., Replogle, J.M., Gilbert, L.A., Villalta, J.E., Torigoe, S.E., Tjian, R., and Weissman, J.S. (2016). Nucleosomes impede Cas9 access to DNA in vivo and in vitro. eLife *5*, e12677.

17. Oh, S.A., Senger, K., Madireddi, S., Akhmetzyanova, I., Ishizuka, I.E., Tarighat, S., Lo, J.H., Shaw, D., Haley, B., and Rutz, S. (2022). High-efficiency nonviral CRISPR/Cas9-mediated gene editing of human T cells using plasmid donor DNA. J. Exp. Med. *219*, e20211530.

18. Balke-Want, H., Keerthi, V., Gkitsas, N., Mancini, A.G., Kurgan, G.L., Fowler, C., Xu, P., Liu, X., Asano, K., Patel, S., et al. (2023). Homology-independent targeted insertion (HITI) enables guided CAR knock-in and efficient clinical scale CAR-T cell manufacturing. Mol. Cancer *22*, 100.

19. Webber, B.R., Johnson, M.J., Skeate, J.G., Slipek, N.J., Lahr, W.S., DeFeo, A.P., Mills, L.J., Qiu, X., Rathmann, B., Diers, M.D., et al. (2024). Cas9-induced targeted integration of large DNA payloads in primary human T cells via homology-mediated end-joining DNA repair. Nat. Biomed. Eng. *8*, 1553–1570. https://doi.org/10.1038/s41551-023-01157-4.

20. Foy, S.P., Jacoby, K., Bota, D.A., Hunter, T., Pan, Z., Stawiski, E., Ma, Y., Lu, W., Peng, S., Wang, C.L., et al. (2023). Non-viral precision T cell receptor replacement for personalized cell therapy. Nature *615*, 687–696.

21. Jing, R., Jiao, P., Chen, J., Meng, X., Wu, X., Duan, Y., Shang, K., Qian, L., Huang, Y., Liu, J., et al. (2021). Cas9-Cleavage Sequences in Size-Reduced Plasmids Enhance Nonviral Genome Targeting of CARs in Primary Human T Cells. Small Methods *5*, e2100071.

22. Tommasi, A., Cappabianca, D., Bugel, M., Gimse, K., Lund-Peterson, K., Shrestha, H., Arutyunov, D., Williams, J.A., Police, S.R., Indurthi, V., et al. (2025). Efficient nonviral integration of large transgenes into human T cells using Cas9-CLIPT. Mol. Ther. Methods Clin. Dev. *33*, 101437.

23. Roth, T.L., Puig-Saus, C., Yu, R., Shifrut, E., Carnevale, J., Li, P.J., Hiatt, J., Saco, J., Krystofinski, P., Li, H., et al. (2018). Reprogramming human T cell function and specificity with non-viral genome targeting. Nature *559*, 405–409.

24. Nguyen, D.N., Roth, T.L., Li, P.J., Chen, P.A., Apathy, R., Mamedov, M.R., Vo, L.T., Tobin, V.R., Goodman, D., Shifrut, E., et al. (2020). Polymer-stabilized Cas9 nanoparticles and modified repair templates increase genome editing efficiency. Nat. Biotechnol. *38*, 44–49.

25. Schober, K., Müller, T.R., Gökmen, F., Grassmann, S., Effenberger, M., Poltorak, M., Stemberger, C., Schumann, K., Roth, T.L., Marson, A., and Busch, D.H. (2019). Orthotopic replacement of T-cell receptor α- and β-chains with preservation of near-physiological T-cell function. Nat. Biomed. Eng. *3*, 974–984.

26. Odé, Z., Condori, J., Peterson, N., Zhou, S., and Krenciute, G. (2020). CRISPR-Mediated Non-Viral Site-Specific Gene Integration and Expression in T Cells: Protocol and Application for T-Cell Therapy. Cancers (Basel) *12*, 1704.

27. Mueller, K.P., Piscopo, N.J., Forsberg, M.H., Saraspe, L.A., Das, A., Russell, B., Smerchansky, M., Cappabianca, D., Shi, L., Shankar, K., et al. (2022). Production and characterization of virus-free, CRISPR-CAR T cells capable of inducing solid tumor regression. J. Immunother. Cancer *10*, e004446.

28. Kath, J., Du, W., Pruene, A., Braun, T., Thommandru, B., Turk, R., Sturgeon, M.L., Kurgan, G.L., Amini, L., Stein, M., et al. (2022). Pharmacological interventions enhance virus-free generation of TRAC-replaced CAR T cells. Mol. Ther. Methods Clin. Dev. *25*, 311–330.

29. Kath, J., Du, W., Martini, S., Elsallab, M., Franke, C., Hartmann, L., Drosdek, V., Glaser, V., Stein, M., Schmueck-Henneresse, M., et al. (2023). CAR NK-92 cell-mediated depletion of residual TCR+ cells for ultra-pure allogeneic TCR-deleted CAR T-cell products. Blood Adv. *7*, 4124–4134. https://doi.org/10.1182/bloodadvances.2022009397.

30. Schumann, K., Lin, S., Boyer, E., Simeonov, D.R., Subramaniam, M., Gate, R.E., Haliburton, G.E., Ye, C.J., Bluestone, J.A., Doudna, J.A., and Marson, A. (2015). Generation of knock-in primary human T cells using Cas9 ribonucleoproteins. Proc. Natl. Acad. Sci. USA *112*, 10437–10442.

31. Quadros, R.M., Miura, H., Harms, D.W., Akatsuka, H., Sato, T., Aida, T., Redder, R., Richardson, G.P., Inagaki, Y., Sakai, D., et al. (2017). Easi-CRISPR: a robust method for one-step generation of mice carrying conditional and insertion alleles using long ssDNA donors and CRISPR ribonucleoproteins. Genome Biol. *18*, 92.

32. Park, S.H., Lee, C.M., Dever, D.P., Davis, T.H., Camarena, J., Srifa, W., Zhang, Y., Paikari, A., Chang, A.K., Porteus, M.H., et al. (2019). Highly efficient editing of the β-globin gene in patient-derived hematopoietic stem and progenitor cells to treat sickle cell disease. Nucleic Acids Res. *47*, 7955–7972.

33. Mabuchi, A., Hata, S., Genova, M., Tei, C., Ito, K.K., Hirota, M., Komori, T., Fukuyama, M., Chinen, T., Toyoda, A., and Kitagawa, D. (2023). ssDNA is not superior to dsDNA as long HDR donors for CRISPR-mediated endogenous gene tagging in human diploid RPE1 and HCT116 cells. BMC Genom. *24*, 289.

34. Shy, B.R., Vykunta, V.S., Ha, A., Talbot, A., Roth, T.L., Nguyen, D.N., Pfeifer, W.G., Chen, Y.Y., Blaeschke, F., Shifrut, E., et al. (2023). High-yield genome engineering in primary cells using a hybrid ssDNA repair template and small-molecule cocktails. Nat. Biotechnol. *41*, 521–531.

35. Jiang, F., and Doudna, J.A. (2017). CRISPR-Cas9 Structures and Mechanisms. Annu. Rev. Biophys. *46*, 505–529.

36. Jinek, M., Chylinski, K., Fonfara, I., Hauer, M., Doudna, J.A., and Charpentier, E. (2012). A programmable dual RNA-guided DNA endonuclease in adaptive bacterial immunity. Science *337*, 816–821.

37. Mali, P., Yang, L., Esvelt, K.M., Aach, J., Guell, M., DiCarlo, J.E., Norville, J.E., and Church, G.M. (2013). RNA-guided human genome engineering via Cas9. Science *339*, 823–826.

38. Zetsche, B., Gootenberg, J.S., Abudayyeh, O.O., Slaymaker, I.M., Makarova, K.S., Essletzbichler, P., Volz, S.E., Joung, J., van der Oost, J., Regev, A., et al. (2015). Cpf1 is a single RNA-guided endonuclease of a Class 2 CRISPR-Cas system. Cell *163*, 759–771.

39. Strohkendl, I., Saifuddin, F.A., Rybarski, J.R., Finkelstein, I.J., and Russell, R. (2018). Kinetic Basis for DNA Target Specificity of CRISPR-Cas12a. Mol. Cell *71*, 816–824.e3.

40. Kleinstiver, B.P., Tsai, S.Q., Prew, M.S., Nguyen, N.T., Welch, M.M., Lopez, J.M., McCaw, Z.R., Aryee, M.J., and Joung, J.K. (2016). Genome-wide specificities of CRISPR-Cas Cpf1 nucleases in human cells. Nat. Biotechnol. *34*, 869–874.

41. Kim, D., Kim, J., Hur, J.K., Been, K.W., Yoon, S.H., and Kim, J.-S. (2016). Genome-wide analysis reveals specificities of Cpf1 endonucleases in human cells. Nat. Biotechnol. *34*, 863–868.

42. Bin Moon, S., Lee, J.M., Kang, J.G., Lee, N.-E., Ha, D.-I., Kim, D.Y., Kim, S.H., Yoo, K., Kim, D., Ko, J.-H., and Kim, Y.S. (2018). Highly efficient genome editing by CRISPR-Cpf1 using CRISPR RNA with a uridinylate-rich 3′-overhang. Nat. Commun. *9*, 3651.

43. Zhang, L., Zuris, J.A., Viswanathan, R., Edelstein, J.N., Turk, R., Thommandru, B., Rube, H.T., Glenn, S.E., Collingwood, M.A., Bode, N.M., et al. (2021). AsCas12a ultra nuclease facilitates the rapid generation of therapeutic cell medicines. Nat. Commun. *12*, 3908.

44. Li, B., Yan, J., Zhang, Y., Li, W., Zeng, C., Zhao, W., Hou, X., Zhang, C., and Dong, Y. (2020). CRISPR-Cas12a Possesses Unconventional DNase Activity that Can Be Inactivated by Synthetic Oligonucleotides. Mol. Ther. Nucleic Acids *19*, 1043–1052.

45. Chen, J.S., Ma, E., Harrington, L.B., Da Costa, M., Tian, X., Palefsky, J.M., and Doudna, J.A. (2018). CRISPR-Cas12a target binding unleashes indiscriminate single-stranded DNase activity. Science *360*, 436–439.

46. Kaminski, M.M., Alcantar, M.A., Lape, I.T., Greensmith, R., Huske, A.C., Valeri, J. A., Marty, F.M., Klämbt, V., Azzi, J., Akalin, E., et al. (2020). A CRISPR-based assay for the detection of opportunistic infections post-transplantation and for the monitoring of transplant rejection. Nat. Biomed. Eng. *4*, 601–609.

47. Wimberger, S., Akrap, N., Firth, M., Brengdahl, J., Engberg, S., Schwinn, M.K., Slater, M.R., Lundin, A., Hsieh, P.-P., Li, S., et al. (2023). Simultaneous inhibition of DNA-PK and Polϴ improves integration efficiency and precision of genome editing. Nat. Commun. *14*, 4761.

48. Karasu, M.E., Toufektchan, E., Chen, Y., Albertelli, A., Cullot, G., Maciejowski, J., and Corn, J.E. (2024). Removal of TREX1 activity enhances CRISPR–Cas9-mediated homologous recombination. Nat. Biotechnol. https://doi.org/10.1038/s41587-024-02356-3.

49. Zhang, S., Wang, Y., Mao, D., Wang, Y., Zhang, H., Pan, Y., Wang, Y., Teng, S., and Huang, P. (2023). Current trends of clinical trials involving CRISPR/Cas systems. Front. Med. *10*, 1292452.

50. Jeon, Y., Choi, Y.H., Jang, Y., Yu, J., Goo, J., Lee, G., Jeong, Y.K., Lee, S.H., Kim, I.-S., Kim, J.-S., et al. (2018). Direct observation of DNA target searching and cleavage by CRISPR-Cas12a. Nat. Commun. *9*, 2777.

51. Romani, A.M.P. (2011). CELLULAR MAGNESIUM HOMEOSTASIS. Arch. Biochem. Biophys. *512*, 1–23.

52. Matsui, Y., Funato, Y., Imamura, H., Miki, H., Mizukami, S., and Kikuchi, K. (2017). Visualization of long-term Mg2+ dynamics in apoptotic cells using a novel targetable fluorescent probe. Chem. Sci. *8*, 8255–8264.

53. Marino, N.D., Pinilla-Redondo, R., and Bondy-Denomy, J. (2022). CRISPR-Cas12a targeting of ssDNA plays no detectable role in immunity. Nucleic Acids Res. *50*, 6414–6422.

54. Fuchs, R.T., Curcuru, J., Mabuchi, M., Yourik, P., and Robb, G.B. (2019). Cas12a trans-cleavage can be modulated in vitro and is active on ssDNA, dsDNA, and RNA. Preprint at bioRxiv. https://doi.org/10.1101/600890.

55. Pohar, J., Lainšček, D., Ivičak-Kocjan, K., Cajnko, M.-M., Jerala, R., and Benčina, M. (2017). Short single-stranded DNA degradation products augment the activation of Toll-like receptor 9. Nat. Commun. *8*, 15363.

56. Unterholzner, L., Keating, S.E., Baran, M., Horan, K.A., Jensen, S.B., Sharma, S., Sirois, C.M., Jin, T., Latz, E., Xiao, T.S., et al. (2010). IFI16 is an innate immune sensor for intracellular DNA. Nat. Immunol. *11*, 997–1004.

57. Wakimoto, Y., Jiang, J., and Wakimoto, H. (2014). Isolation of Single-Stranded DNA. Curr. Protoc. Mol. Biol. *107*. 15.1-2.15.9.

58. Veneziano, R., Shepherd, T.R., Ratanalert, S., Bellou, L., Tao, C., and Bathe, M. (2018). In vitro synthesis of gene-length single-stranded DNA. Sci. Rep. *8*, 6548.

59. Iyer, S., Mir, A., Vega-Badillo, J., Roscoe, B.P., Ibraheim, R., Zhu, L.J., Lee, J., Liu, P., Luk, K., Mintzer, E., et al. (2022). Efficient Homology-Directed Repair with Circular Single-Stranded DNA Donors. CRISPR J. *5*, 685–701.

60. Richardson, C.D., Kazane, K.R., Feng, S.J., Zelin, E., Bray, N.L., Schäfer, A.J., Floor, S. N., and Corn, J.E. (2018). CRISPR–Cas9 genome editing in human cells occurs via the Fanconi anemia pathway. Nat. Genet. *50*, 1132–1139.

61. Kanke, K.L., Rayner, R.E., Bozik, J., Abel, E., Venugopalan, A., Suu, M., Nouri, R., Stack, J.T., Guo, G., Vetter, T.A., et al. (2024). Single-stranded DNA with internal base modifications mediates highly efficient knock-in in primary cells using CRISPR-Cas9. Nucleic Acids Res. *52*, 13561–13576.

62. Nam, H., Xie, K., Majumdar, I., Yang, S., Starzyk, J., Lee, D., Shan, R., Li, J., and Wu, H. (2023). Engineering Tripartite Gene Editing Machinery for Highly Efficient Non-Viral Targeted Genome Integration. Res. Sq. *23*, rs.3.rs-3365585. https://doi.org/10.21203/rs.3.rs-3365585/v1.

63. Foss, D.V., Muldoon, J.J., Nguyen, D.N., Carr, D., Sahu, S.U., Hunsinger, J.M., Wyman, S.K., Krishnappa, N., Mendonsa, R., Schanzer, E.V., et al. (2023). Peptide-mediated delivery of CRISPR enzymes for the efficient editing of primary human lymphocytes. Nat. Biomed. Eng. *7*, 647–660.

64. Zhang, Z., Baxter, A.E., Ren, D., Qin, K., Chen, Z., Collins, S.M., Huang, H., Komar, C.A., Bailer, P.F., Parker, J.B., et al. (2024). Efficient engineering of human and mouse primary cells using peptide-assisted genome editing. Nat. Biotechnol. *42*, 305–315.

65. Wiebking, V., Lee, C.M., Mostrel, N., Lahiri, P., Bak, R., Bao, G., Roncarolo, M. G., Bertaina, A., and Porteus, M.H. (2021). Genome editing of donor-derived T-cells to generate allogenic chimeric antigen receptor-modified T cells: Optimizing αβ T cell-depleted haploidentical hematopoietic stem cell transplantation. Haematologica *106*, 847–858.

66. Allen, A.G., Khan, S.Q., Margulies, C.M., Viswanathan, R., Lele, S., Blaha, L., Scott, S. N., Izzo, K.M., Gerew, A., Pattali, R., et al. (2024). A highly efficient transgene knock-in technology in clinically relevant cell types. Nat. Biotechnol. *42*, 458–469.

67. Du, W., Noyan, F., McCallion, O., Drosdek, V., Kath, J., Glaser, V., Fuster-Garcia, C., Yang, M., Stein, M., Weber, O., et al. (2024). Gene editing of CD3 epsilon gene to redirect regulatory T cells for adoptive T cell transfer. Preprint at bioRxiv. https://doi.org/10.1101/2024.03.18.584896.

68. Cullot, G., Aird, E.J., Schlapansky, M.F., Yeh, C.D., van de Venn, L., Vykhlyantseva, I., Kreutzer, S., Mailänder, D., Lewków, B., Klermund, J., et al. (2024). Genome editing with the HDR-enhancing DNA-PKcs inhibitor AZD7648 causes large-scale genomic alterations. Nat. Biotechnol. https://doi.org/10.1038/s41587-024-02488-6.